Plant Physiol. (1990) 92, 103–109
0032-0889/90/92/0103/07/$01.00/0

Received for publication February 29, 1989
and in revised form August 3, 1989

Leaf Cuticles Behave as Asymmetric Membranes[1]

Evidence from the Measurement of Diffusion Potentials

Melvin T. Tyree*, Timothy D. Scherbatskoy, and Christopher A. Tabor

Northeastern Forest Experiment Station, P. O. Box 968, Burlington, Vermont 05402 (M.T.T., C.A.T.); *and Botany Department, University of Vermont, Burlington, Vermont 05405* (M.T.T., T.D.S.)

ABSTRACT

Cuticles were isolated enzymatically from the leaves of two maple species (*Acer saccharum* Marsh and *A. platanoides* L.) and from orange (*Citrus aurantium* L.). The cuticles were placed in a plastic cuvette and different concentrations of KCl were perfused over the physiological inner and outer surfaces while the electrical potential (E^{io}) that developed across the cuticles and was caused by ion diffusion was measured. E^{io} was always positive, indicating that the permeability of K^+ was always greater than that of Cl^-. Measured E^{io} in cuticles did not fit the Goldman equation, whereas, E^{io} measured during KCl diffusion across selected artificial membranes fit the equation. The magnitude of E^{io} in cuticles and artificial membranes also was dependent on ionic strength, decreasing as ionic strength increased. These observations are explained by combining classical transport equations with equations that describe the equilibrium ion distribution between ionic double layers in the cuticle or membranes and the bathing solution.

Relatively little is known about the mechanism of ion permeation through leaf cuticles. More is known about the permeation of nonelectrolytes. On the basis of permeation studies and thermodynamic arguments, Schönherr (6, 7) concluded that small nonelectrolytes permeate through cuticular pores of up to 0.9 nm in diameter. Since the hydrated diameter of many ions is less than 0.8 nm, it is highly probable that ions also permeate through these pores. Schönherr (6) calculated that pores number about 10^{10} pores cm^{-2} of cuticle surface, and they occupy about 6 ppm of the surface area of cuticles. When chloroform-soluble cuticular lipids were extracted, leaving only the cuticular matrix, water permeability increased by two to three orders of magnitude, suggesting 100 to 1000 times more pores were exposed by removal of cuticular lipids.

Schönherr and Bukovac (8, 9) demonstrated that cuticular pores also have polar regions composed of the following components: (a) polyuronic acids associated with cellulose and pectin in the secondary cuticle, (b) cutin, which is a weakly polar compound due to hydroxyl and unesterified carboxyl groups, and (c) certain cuticular waxes with polar substituents. Since the bulk of a cuticle consists of nonpolar substances, it is reasonable to expect the polar substituents would aggregate during cuticle synthesis to achieve the most stable (*i.e.* lowest energy) molecular structures. This thermodynamic process will tend to create pores with an unusually high concentration of polar groups and cation exchange sites. Diffusion through polar pores probably explains why electrical potentials ('diffusion potentials') arise when salts are made to diffuse across isolated cuticles. So far, diffusion potentials have been measured only as a way to measure the pH of the isoelectric point of cuticles (10).

For this paper, we measured the diffusion potential of KCl solutions across isolated cuticles and use this method to test the polar pore model. The following standard theory is assumed to apply.

The flux of ions is determined by both a concentration difference and an electrical potential difference. If we assume that the electrical potential gradient is constant through the membrane (the so called constant field assumption), then we can use the following equation to describe flux of the jth ionic species (4, Chapter 3):

$$J_j = -P_j \frac{x}{1 - e^x} (C_j^o - C_j^i e^x) \qquad (1)$$

where J is the ion flux, P is the permeability, C is concentration, the subscript j refers to the jth ionic species, the superscripts i and o refer to the inside and outside solutions, respectively, on either side of the membrane, and $x = z_j F E^{io}/RT$ where z is the valence, F is the Faraday constant, R is the gas constant, T is the absolute temperature, and E^{io} is the electrical potential difference across the membrane with the outside taken as ground. When KCl diffuses across a cuticle, the fluxes of the anion and cation must be equal ($J_K = J_{Cl}$) if there is to be no long term charge accumulation. Setting these fluxes equal and writing Equation 1 for each case, and solving the equations for E^{io}, yield the Goldman equation (2),

$$E^{io} = \frac{F}{RT} \ln \frac{P_K[K]^o + P_{Cl}[Cl]^i}{P_K[K]^i + P_{Cl}[Cl]^o} = \frac{F}{RT} \ln \frac{(1 + P_R C_R)}{C_R + P_R} \qquad (2)$$

where in the first ln term P_K and P_{Cl} are the permeabilities of K^+ and Cl^-, respectively, and where [ ] means concentration of the ion indicated on the inside (superscript i) or outside (superscript o), respectively. The second ln term is more suited to curve fitting and is obtained by dividing numerator and

[1] This research was supported by funds from the U.S. Department of Agriculture, U.S. Forest Service, Northeastern Forest Experiment Station, and by grant numbers USDA 87-CRSR-2-3021 and USDA 88-34157-3748.

denominator of the first ln term by $P_K[K]^o$ and replacing $[K]^o = [Cl]^o$ with C^o and similarly $[K]^i = [Cl]^i$ with C^i. P_R is the ratio of permeabilities (P_{Cl}/P_K) and C_R is the ratio of KCl concentrations (C^i/C^o).

In both Equations 1 and 2 it can be shown that permeability can be related to more fundamental quantities,

$$P_j = u_j K_j RT/\Delta x \quad (3)$$

where K is the partition coefficient, u is the mobility, and Δx is the thickness of the membrane. To derive Equations 1 and 2, it is necessary to assume that K_j and P_j both remain constant across the membrane. Also it is assumed that the electric field in the membrane is constant, *i.e.* the voltage changes linearly with distance. In the course of our research, we began to suspect that none of these assumptions is met in cuticles or in other membranes we studied. Nevertheless, there still is value in retaining the above theory because deviations of our results from theory can be explained in terms of deviation from underlying assumptions. A final assumption that is made in Equation 2 is that the electric potential arises only from passive diffusion processes. This assumption is rarely met in biological membranes, and deviations from Equation 2 are usually explained in terms of ion pumps in living membrane systems. In our case, we can rule out the presence of ion pumps, so deviations must be explained in terms of failure to meet the first three assumptions.

MATERIALS AND METHODS

Cuticle Isolation

Leaves of field-grown sugar maple (*Acer saccharum* Marsh.), Norway maple (*Acer platanoides* L.), and greenhouse-grown sour orange (*Citrus aurantium* L.) were used in the experiments described here. Leaves were lightly abraded on the abaxial surface with 120-grit sandpaper to facilitate entry of enzyme solution. Discs (14 mm diameter) were cut from each leaf, avoiding major veins, and were placed in flasks containing filtered pectinase and cellulase (both from ICN Biochemicals, Cleveland, OH) in 0.1 M Na-Acetate buffer at pH 3.7 (5). Concentrations of these enzymes varied with species being isolated. *Citrus* cuticles could be isolated in 1 to 3 d using a solution of 10% pectinase and 1% cellulase (w/v). *Acer* cuticles, which were difficult to isolate, required 20% pectinase and 2% cellulase, and an incubation time of 1 to 2 weeks. Pectinase alone (20%) was ineffective and cellulase above 2% did not speed isolation. The addition of up to 5% hemicellulase did not improve cuticle isolation.

Leaf discs were incubated at 37°C. Enzyme solutions were replaced weekly, and 1 mM NaN_3 was added to suppress microbial growth. Cuticles were removed by gently teasing them away from the underlying leaf matrix with a spatula. They were rinsed in deionized water, soaked 10 min in each of three aliquots of 1 N HCl to saturate exchange sites with H^+, and rinsed with deionized water. Isolated cuticles were stored at room temperature in deionized water.

A scanning electron microscope was used to examine the adaxial surfaces of intact leaves and of cuticles isolated from them. We observed little change in the crystalline structure of surface waxes between isolated cuticles and those on intact leaves.

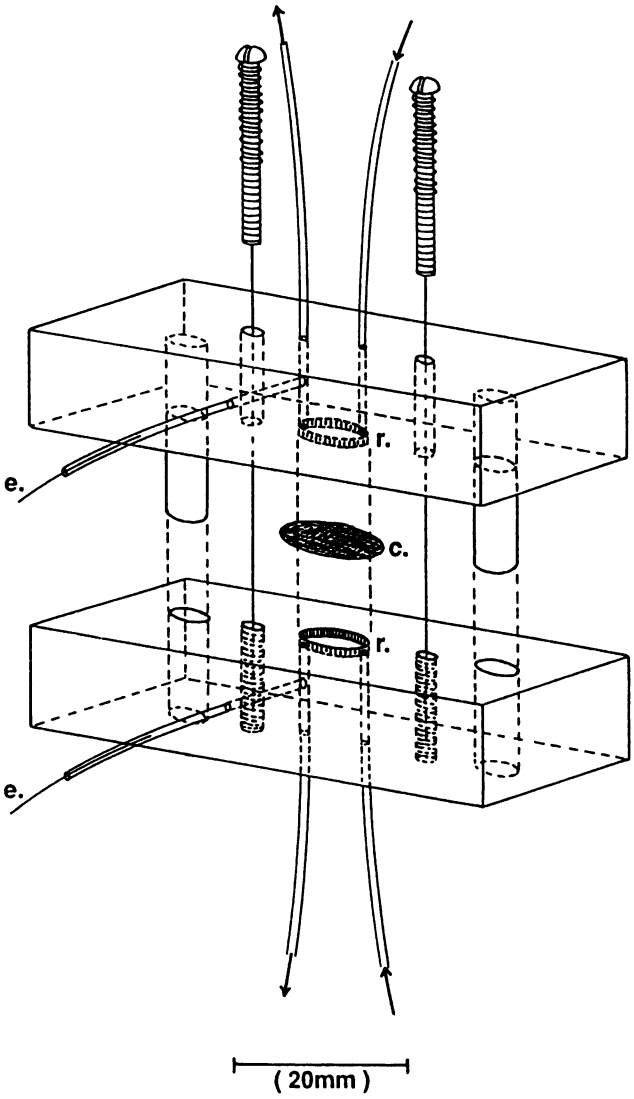

Figure 1. Apparatus used to hold cuticle membrane (*c*) while solutions are pumped across its two faces. Arrows denote inflow and outflow in a reservoir (*r*) that is 6 mm in diameter and 1 mm deep; electrodes (*e*) are inserted into outflow ports.

Artificial Membranes

Diffusion potentials were also measured in a selection of other artificial membranes. These included: (a) Spectra/Por 3 dialysis membrane (Spectrum Medial Industries Inc., Los Angeles, CA) which was composed of cotton cellulose, 0.05 mm thick, with a nominal mol wt cutoff of 3500; (b) the blue spacer papers from two lots of Millipore filters (lot A = GSWP 02500 No. H7C81457A and lot B = HATF 047X No. H2E68397A), and (c) Crane's Thesis Paper of 100% rag content (No. 26-133).

Electrical Measurements

Adaxial cuticles or other membranes were placed between the two halves of a flow cell (Fig. 1). Silicone stopcock grease (Dow Corning High Vacuum) was used to provide a seal. Cuticles were floated into place in deionized water or dried for about 1 h on a Teflon screen and then placed in the flow cell. Unbuffered solutions of reagent grade KCl were prepared in deionized water. Various concentrations of these salt solutions were simultaneously pumped across the two sides of the cuticle to create ion concentration gradients across the cuticle. Solutions were pumped with an Ismatec peristaltic pump (Cole-Parmer No. 7618-40), first at a fast rate (1.2 mL min^{-1}) for 90 s to completely exchange solutions, then at a slow rate (0.2 mL min^{-1}) for 90 s for equilibration.

Salt-bridge electrodes were inserted in the outflow of each half-cell (Fig. 1) to measure electrical potential difference across the cuticle. These electrodes consisted of Ag-AgCl wire (0.25 mm diameter) in 0.4 mm i.d. polypropylene tubing filled with 100 mM KCl in 0.4% agarose. Electrical signals were amplified through an electrometer (WP Instruments model 725, New Haven, CT), monitored on a digital multimeter with a precision of 0.1 mV, and recorded on a chart recorder. Cuticles were mounted so that the physiological outer surface was facing the grounded electrode. Thus, the voltage measured, E^{io}, was that at the physiological inner surface relative to ground. Electrical measurements were made while pumping solution at 0.2 mL min^{-1} or often with the pump briefly turned off since this reduced the electrical noise but did not change the reading. Electrical measurements were made in a Faraday cage to reduce electrical noise. All experiments were conducted at temperatures within the range 22 to 26°C.

Diffusion potentials were measured under three experimental regimes:

1. *Varying Ionic Strength and Concentration Ratios.* One side of the membrane was maintained at 100 mM KCl while the concentration on the other side was varied to provide ratios C_R between 0.01 and 100.

2. *Constant Ionic Strength and Varying Concentration Ratios.* One average ionic strength within the membrane (calculated as $(C^i + C^o)/2$) was maintained at 10 mM KCl while C_R ranged from 0.01 to 100.

3. *Varying Ionic Strengths and Constant Concentration Ratios.* The C_R was maintained at 10 or 0.1 while the ionic strength (calculated as $(C^i + C^o)/2$) ranged from 55 to 0.55 mM (*i.e.* C^i/C^o = 100/10 to 1/0.1).

RESULTS

Substantial electrical potentials (E^{io} up to ±120 mV) developed across isolated cuticles exposed to varying KCl concentration ratios (C_R) with and without ionic strength constant. These potentials became increasingly positive or negative as C_R decreased or increased, respectively, from unity. This is clearly seen for all cuticles; see, for example, Figure 2, A, B, and C, where the ionic strength varied, and Figure 3, A, B, and C, where the ionic strength was constant. E^{io}s of large magnitude indicate that K^+ is more permeable than Cl^- (low permeability ratio, P_R). The most striking feature of these

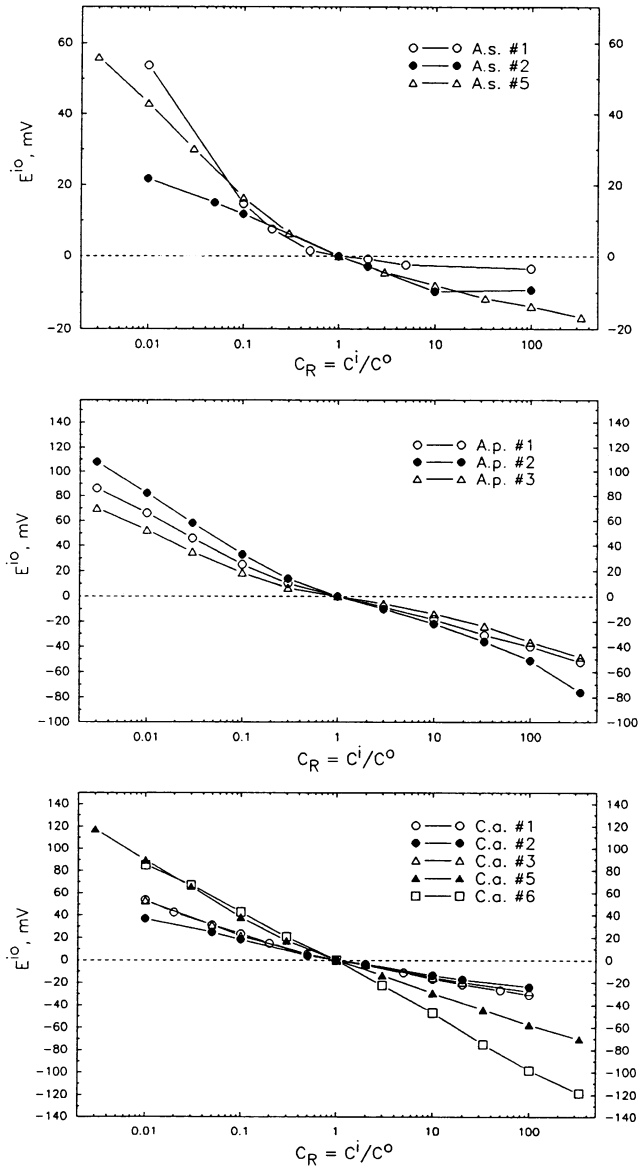

Figure 2. Diffusion potentials (E^{io}) for isolated cuticles of *Acer saccharum* (A.s.), *A. platanoides* (A.p.), and *Citrus aurantium* (C.a.) membranes exposed to KCl concentration ratios (C_R) with one side kept at 100 mM. Each plot represents measurements on a single cuticle, as indicated in the legend. Both C_R and ionic strength vary in these experiments.

data is the lack of symmetry around $C_R = 1$. Because C_Rs <1 and >1 are simply the result of reversing the orientation of the solutions with respect to the cuticle, one would expect potentials of equal magnitude and opposite polarity around $C_R = 1$. This was not the case. Potentials with $C_R < 1$ usually were substantially larger in magnitude than when $C_R > 1$. In Figures 2A and 3A, positive potentials ($C_R < 1$) were sometimes three times the magnitude of the corresponding negative potential for the same cuticle. The degree of the asymmetry varied from cuticle to cuticle.

The magnitude of E^{io} measured under constant C_R also was a function of ionic strength in isolated cuticles (Fig. 4). In

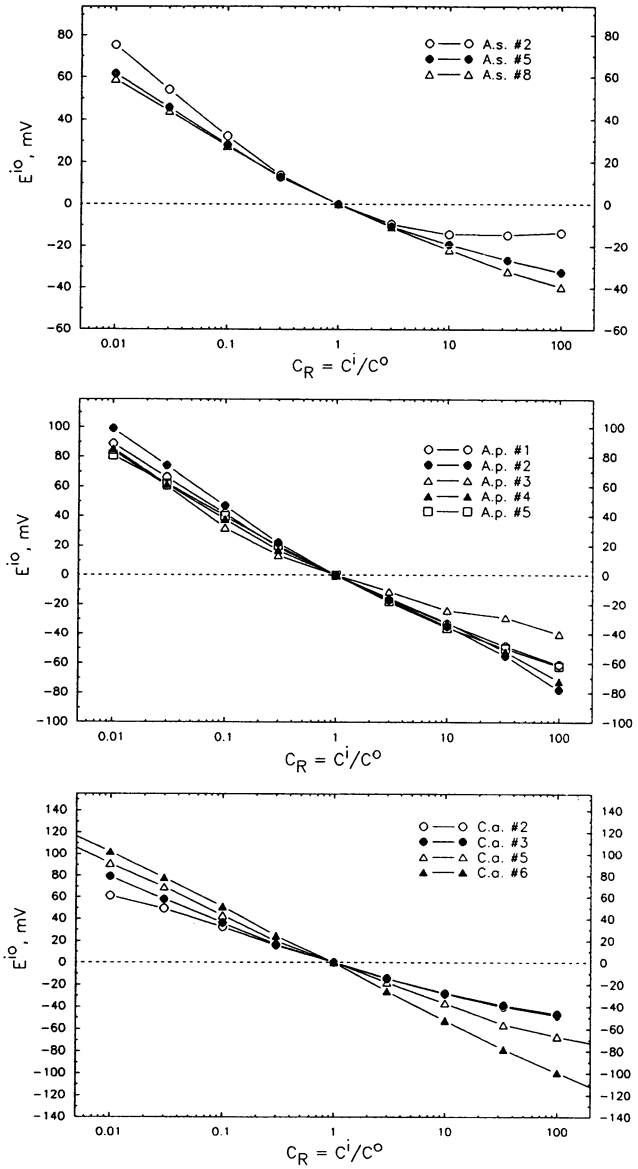

Figure 3. Similar to Figure 2 except ionic strength is constant at 10 mM while C_R varies.

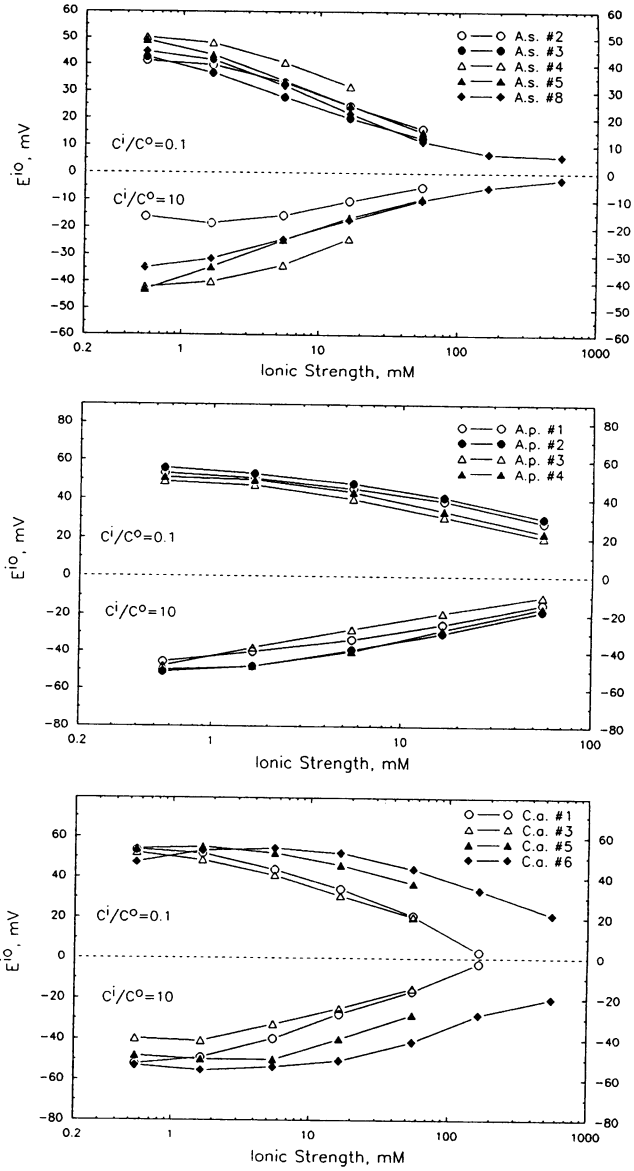

Figure 4. Similar to Figure 2 except C_R is constant at 10 or 0.1 while ionic strength varies.

these experiments, the C_Rs were equal to 0.1 or 10 (which should simply change the polarity of the measured E^{io}); however, as the ionic strength decreased, E^{io} increased in magnitude. The maximum magnitude of E^{io} observed was nearly ±59 mV, which is what should occur in the limiting case where P_R approaches zero. At 1 mM, E^{io} typically equaled ±50 mV and this corresponds to a P_R of 0.0402. As ionic strength increased above 1 mM, E^{io}s decreased in magnitude. At an E^{io} of ±5 mV, the predicted P_R equaled 0.786. At low ionic strength, the asymmetry between the magnitude of E^{io} at C_R = 10 *versus* that at C_R = 0.1 tended to decrease. The asymmetry was most pronounced at intermediate ionic strengths (20–200 mM).

The Goldman equation (2) is a symmetric equation; that is, the computed E^{io}s will be $+x$ or $-x$ for C_R of y or $1/y$, respectively. We measured diffusion potentials in a variety of artificial membranes and found four types (those listed in "Materials and Methods") to be symmetric. Representative results for paper from lot A are shown in Figure 5, A, B, and C. All four types of artificial membranes (data not shown) were symmetric but differed in the magnitude of the measured E^{io} *versus* C_R, or *versus* ionic strength. The data in Figure 5, A and B, were fitted to Equation 2 by a least squares procedure; the best fit occurred at P_R = 0.698 in Figure 5A and at P_R = 0.352 in Figure 5B. The closeness of fit was not as good in Figure 5A as in Figure 5B; however, this can be attributed to the strong dependence of E^{io} on ionic strength (Fig. 5C). In Figure 5B ionic strength was constant, but in Figure 5A the ionic strength was 100 mM at C_R = 1 and decreased to 55 at both extremes of C_R. The direction of the deviations were as would be expected for the change in ionic strength. Numbers next to the open circles in Figure 4C are the permeability ratios computed from Equation 2 at each ionic strength.

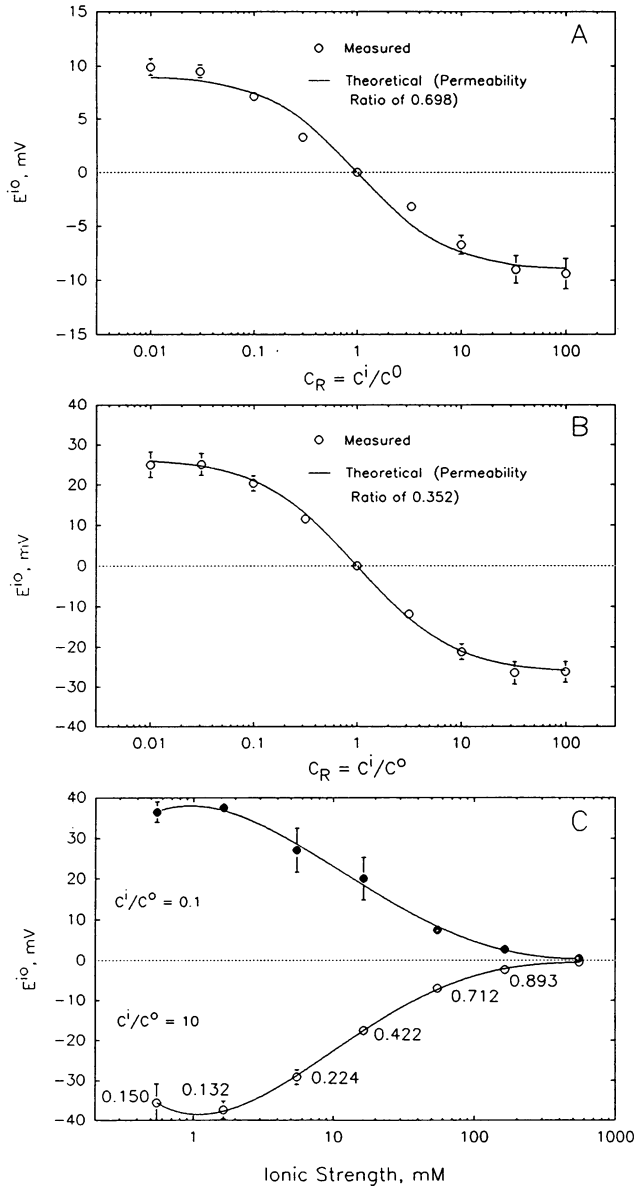

Figure 5. Diffusion potentials (E^{io}) for Millipore spacer paper (lot A) membranes exposed to KCl solutions. A, Concentration ratio (C_R) varies while one side kept at 100 mM; B, ionic strength kept constant at 10 mM while C_R varies; C, C_R is constant at 10 or 0.1 while ionic strength varies. Curves drawn through A and B are least squares fits of the Goldman equation (2) to the experimental data. Each point is the mean of five membranes. Error bars (standard deviation) are drawn when bigger than the symbol size.

Experiments such as the one in Figure 5 were repeated for Crane's 100% rag paper and for another production lot of Millipore spacing paper (lot B). Results were similar to those in Figure 5B except for the magnitude of the measured E^{io}, which translates directly into differences in P_R which equaled 0.505 and 0.150 for the Crane's paper and lot B, respectively. Figure 6 shows the result of constructing an artificial asymmetric membrane from a bilayer of one sheet of lot B paper and one sheet of Crane's paper. The bilayer was a model for a cuticle in which lot B paper was designated the inner surface

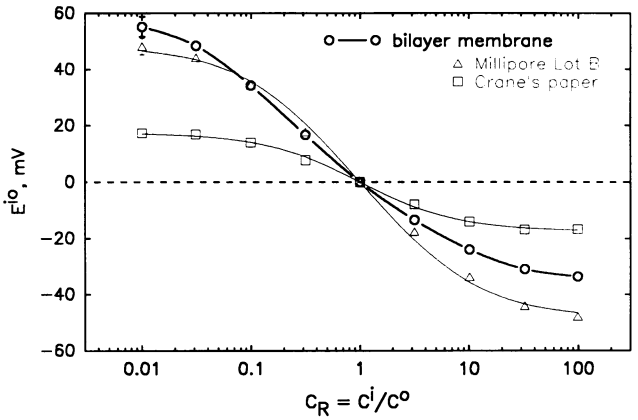

Figure 6. Diffusion potentials (E^{io}) for Millipore spacer paper (lot B) and for Crane's paper and for a bilayer membrane made up of one sheet of each. Concentration ratio (C_R) varied while ionic strength was held constant at 10 mM. Curves drawn through lot B and Crane's paper are the least squares fits of the Goldman equation (2). A smooth curve is drawn through the bilayer data to connect the points but the curve does not come from the Goldman equation. Each point is the mean of five membranes. Error bars (standard deviations) are drawn when bigger than the symbol size.

and the Crane's paper the outer surface. Diffusion potentials measured on this bilayer were asymmetric (Fig. 6).

DISCUSSION

A single model of cuticle and artificial membranes can explain two properties: (a) the dependence of E^{io} (and thus P_R) on ionic strength and (b) why cuticles and the bilayer in Figure 6 show asymmetric properties.

Both the cuticle and artificial membranes are weak-acid, cation-exchange materials. If the fixed-charge distribution were uniform throughout the material, then the simple equations describing classical Donnan equilibria could be used to calculate K^+ and Cl^- equilibrium concentrations between the material and bathing solution. These equilibria in turn could be used to calculate partition coefficients and permeability ratios. The more realistic case, where fixed charges are not distributed uniformly, will be discussed later.

From the Boltzmann equation (11), we have

$$C_K^* C_{Cl}^* = C_K C_{Cl} = C^2 \tag{4}$$

where C_K and C_{Cl} are the concentrations of K^+ and Cl^-, respectively, in the bathing solution and C_K^* and C_{Cl}^* are the corresponding concentrations in the material. Since $C_K = C_{Cl}$, we replace both with C. Since the sum of positive and negative charges inside the material must be equal, we also have

$$C_K^* - C_{Cl}^* = A \tag{5}$$

where A is the average concentration of fixed charges in equivalent per m^3 of material. Also, A is the CEC[2] of the material in equivalent per unit volume rather than the more usual units of equivalent per g dry weight. Solving Equations

[2] Abbreviations: CEC, cation exchange capacity.

4 and 5 simultaneously leads to a quadratic equation with the following solutions:

$$C_K^* = \frac{A + \sqrt{A^2 + 4C^2}}{2}; \quad (6a)$$

$$C_{Cl}^* = \frac{-A + \sqrt{A^2 + 4C^2}}{2}. \quad (6b)$$

Using Equation 3, written explicitly for K^+ and Cl^-, it can be seen that the permeability ratio, $P_R = P_{Cl}/P_K$, is given by $u_{Cl}K_{Cl}/u_KK_K$. It is known that the mobilities of ions in ion exchange materials are close to those in open solution (3), so it is reasonable to assume that the mobilities of K^+ and Cl^- (u_K and u_{Cl}) will be approximately equal in our materials as they are in open solution; therefore, the ratio of partition coefficients will be approximately proportional to the ratio of permeabilities. Dividing Equations (6a) and (6b) by C yields the partition coefficients for K^+ (K_K) and for Cl^- (K_{Cl}). So we have

$$P_R = P_{Cl}/P_K \simeq \frac{(-A + \sqrt{A^2 + 4C^2})}{(A + \sqrt{A^2 + 4C^2})}. \quad (7)$$

Equation 7 predicts that as the concentration of KCl in the bathing solution C approaches zero, P_R will approach zero, and that when $C \gg A$, then $P_R = 1$. This probably explains the dependence of E^{io} on ionic strength in Figures 4 and 5C. At low ionic strength when E^{io} approaches ±59 mV, the Goldman equation (2) would require that P_R approaches 0. At high ionic strength when E^{io} approaches 0, Equation 2 would require that P_R approaches 1.

It is unlikely that the fixed-charge distribution in cuticles or in our artificial membranes is uniform. In a study of the ion exchange properties of isolated cell walls, Dainty and Hope (1) obtained experimental evidence suggesting that cell walls are divided into three volume fractions consisting of a free space (α), a double layer (β), and solids (γ), where $\alpha + \beta + \gamma = 1$. In the free space, soluble anions and cations are of equal concentration as in open solution, whereas, in the double layer, ionic concentrations are determined by the Gouy-Chapman double-layer theory (11). Dainty and Hope (1) show that the more complex Gouy-Chapman formula will predict the same ion distribution as the Donnan formulas for a specific double-layer thickness, δ. The boundary at distance δ divides the region between fixed charges and the bulk solution into a Donnan space and free space. The value of δ decreases with the inverse of the square root of the ionic strength, so the volume fraction β will decrease and α will increase correspondingly. Similar relations could be derived for the more modern Stern-Grahame double-layer model (11), though this was not done by Dainty and Hope (1). With this more realistic model of charge distribution, a slightly more complicated form of Equation 7 results:

$$P_R \simeq \frac{\alpha - \beta(A/2C) + \beta\sqrt{(A/2C)^2 + 1}}{\alpha + \beta(A/2C) + \beta\sqrt{(A/2C)^2 + 1}} \quad (8)$$

where now A is the average concentration of fixed charges in the volume fraction β. Equation 8 has the same limits as Equation 7, that is, $P_R \rightarrow$ O as $C \rightarrow$ O and $P_R \rightarrow 1$ as C $\rightarrow \infty$. We have derived an even more complex equation that applies to a membrane with a large cation-exchange volume fraction β and a smaller anion-exchange volume fraction β' and of concentration B in that volume. The limits of this equation (not shown) are $P_R \rightarrow \beta' B/\beta A$ as $C \rightarrow$ O and $P_R \rightarrow 1$ as $C \rightarrow \infty$.

All else being equal, Equations 7 or 8 also would predict that materials with a high CEC (related to A) would have lower P_R and bigger E^{io}s than a material with low CEC. This would seem to explain the asymmetric behavior of the bilayer membrane in Figure 6 and of cuticles. A symmetrical membrane must have a uniform CEC. When salts diffuse across such a membrane, P_R will change gradually from a high value on the high-concentration side to a low on the low-concentration side. But the range of P_Rs is the same whether $C_R = y$ or $1/y$. In an asymmetric membrane, one in which the CEC is higher near one surface than on the other, this is no longer true. When the higher solution concentration is on the highly charged side of the membrane, the P_R might be reduced below that on the dilute side so there is a low magnitude E^{io}. When the solutions are reversed so that the concentrated side is near the low charged side of the material, the P_R there might increase to near unity; but on the dilute side where the membrane is highly charged, the P_R might be nearly unchanged so there will be a large magnitude E^{io}.

Equations 7 or 8 suggest that CEC membranes (*e.g.* paper) ought not obey the Goldman theory, Equation 2, since the partition coefficient, K_j, and thus the permeability ratio, P_R, are not constant across the membrane. Yet the fit of Equation 2 to the experimental data is remarkably good (Fig. 6). We suggest that the restriction that K_j must remain constant across the membrane cannot be too important for membranes with uniform charge distribution. The P_R required to fit the data must reflect some average ratio near the middle of the membrane. The reason for the observed good fit is not clear to us, and we hope some theoretician will eventually explain our results.

The asymmetric property of cuticles also might be explained in terms of a charged-pore model of transport through cuticles. As ions diffuse through the cuticle, their progress is modified by electrical interactions with the double layer in the pores (shaded area in Fig. 7). High concentrations of mobile cations accumulate adjacent to the fixed anions in the pore; mobile anions are excluded from this region. The thickness of this anion exclusion region (double layer) is sensitive to the external ion concentration, decreasing in thickness as the external ion concentration increases. The thickness of the double layer also is a function of fixed-change density; the greater the charge, the thicker the double layer. Depending on the thickness of the double layer in the pore, the relative permeability of ion pairs will be more or less affected. These relationships are presented schematically in Figure 7, which shows four hypothetical effects of bulk-solution concentration on the thickness of the double layer in cuticular pores. In Figure 7A the double layer is relatively thick in the presence of low ionic concentrations of 1 mM KCl throughout the pore. Because of the asymmetric distribution of fixed anions in the pore, the double layers overlap near the inner side of the cuticle. The high concentrations (10 mM) reduce the dimen-

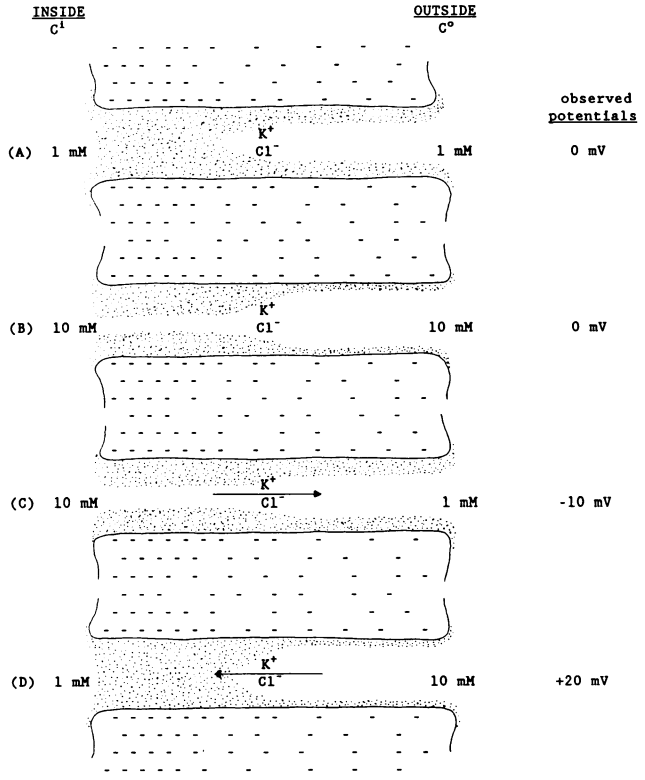

Figure 7. Schematic representation of the influence of ionic concentration on Donnan regions, ion pair diffusion, and diffusion potential in a circular pore. See text for discussion. Not to scale.

sions of the double layers in Figure 7B so that they no longer overlap. As there are no concentration gradients, there are no diffusion potentials under the conditions in Figure 7A, and B. In Figure 7, C and D, we have the possibility of asymmetric diffusion potentials. Although a 10-fold concentration ratio exists in both cases, the diffusion potential is greater in Figure 7D than in Figure 7C. This occurs because the combination of low ionic concentration and high fixed-anion density at the inner side of the cuticular pore produces double layers which more or less occlude this part of the pore. The relative permeability of the diffusion anion is reduced in this anion-exclusion region much more than in Figure 7C.

Structurally, we would expect the cuticle to be more densely charged on the inner than on the outer surface. The inner surface blends in with the cell wall that has an abundance of charged groups (proteins, polyuronic acids, etc.), whereas the outer surface is predominantly uncharged waxes. The results of the bilayer paper membrane (Fig. 6) strongly support this model of ion permeation thorough cuticles.

The techniques we have developed here may prove to be valuable as a measure of the physiological state of cuticles. Diffusion potentials will change with charge density which, in turn, may depend on cuticle ontogeny and/or a number of environmental variables such as UV-B or ozone levels and the relative abundance of acids and other ions in ambient precipitation. Diffusion potentials varied greatly from cuticle to cuticle and species to species in Figures 2, 3, and 4. It is possible that the isolation procedures may have contributed to this variability. The longer the leaves remain in the enzyme solution, one would expect a larger fraction of the cellulose components and charged groups to be removed from the inner surface. More work will be required to determine if these techniques can be useful probes of cuticle physiology. This technique already has provided new insights into the mechanism of ion permeation through cuticles.

LITERATURE CITED

1. **Dainty J, Hope AB** (1961) The electric double layer and the Donnan equilibrium in relation to plant cell walls. Aust J Biol Sci **14:** 541–551
2. **Goldman DE** (1943) Potential, impedance, and rectification in membranes. J Gen Physiol **27:** 37–60
3. **Meares P** (1968) Transport in ion-exchange polymers. *In* J Crank, GS Park, eds, Diffusion in Polymers. Academic Press, London, pp 373–428
4. **Nobel PE** (1983) Biophysical Plant Physiology and Ecology, WH Freeman, New York
5. **Orgell WH** (1955) The isolation of plant cuticle with pectic enzymes. Plant Physiol **30:** 78–80
6. **Schönherr J** (1976) Water permeability of isolated cuticular membranes: the effect of cuticular waxes on diffusion of water. Planta **131:** 159–164
7. **Schönherr J** (1979) Transcuticular movement of xenobiotics. *In* H Geissbuhler, GT Brooks, PC Kearne, eds, Advances in Pesticide Science. Pergamon, Oxford, pp 392–400
8. **Schönherr J, Bukovac MJ** (1970) Preferential polar pathways in the cuticle and their relationship to ectodesmata. Planta **92:** 189–201
9. **Schönherr J, Bukovac JM** (1973) Ion exchange properties of isolated tomato fruit cuticular membrane: exchange capacity, nature of fixed charges and cation selectivity. Planta **109:** 73–93
10. **Schönherr J, Huber R** (1977) Plant cuticles are polyelectrolytes with isoelectric points around three. Plant Physiol **59:** 145–150
11. **Singh U, Uehara G** (1986) Electrochemistry of the double-layer: Principles and applications to soils. *In* DL Sparks, ed, Soil Physical Chemistry, CRC Press, Boca Raton, FL, pp 1–38